Predicting the single-proton and single-neutron potentials in asymmetric nuclear matter

F. Sammarruca, W. Barredo, and P. Krastev
Physics Department, University of Idaho, Moscow, Idaho 83844, USA
(Received 16 December 2004; published 9 June 2005)

We discuss the one-body potentials for protons and neutrons obtained from Dirac-Brueckner-Hartree-Fock calculations of neutron-rich matter, in particular their dependence upon the degree of proton/neutron asymmetry. The closely related symmetry potential is compared with empirical information from the isovector component of the nuclear optical potential.

DOI: 10.1103/PhysRevC.71.064306 PACS number(s): 21.65.+f, 21.30.Fe, 21.60.−n

I. INTRODUCTION

Lately we have been concerned with probing the behavior of the isospin-asymmetric equation of state (EOS). With our recent work on neutron radii and neutron skins [1], we have explored applications of the EOS at densities typical for normal nuclei.

It is also important to look into systems that are likely to constrain the behavior of the EOS at higher densities, where the largest model dependence is observed. Supernova explosions and neutron star formation/stability are phenomena where the nuclear EOS plays a crucial role. The symmetry energy determines the proton fraction in neutron stars in β equilibrium, and, in turn, the cooling rate and neutrino emission. Models of prompt supernova explosion and systematic analyses of neutron star masses provide often conflicting information on the "softness" of the EOS and its incompressibility at equilibrium.

On the other hand, collisions of neutron-rich nuclei, which are the purpose of the Rare Isotope Accelerator (RIA), provide a unique opportunity to obtain terrestrial data suitable for constraining the properties of dense and highly asymmetric matter. Such reactions are capable of producing extended regions of space/time where both the total nucleon density and the neutron/proton asymmetry are large. Isospin-dependent Boltzmann-Uehling-Uhlenbeck (BUU) transport models [2] include isospin-sensitive collision dynamics through the elementary pp, nn, and np cross sections and the mean field. The latter is a crucial isospin-dependent mechanism, and is the focal point of this paper. The contribution to the mean field from the neutron/proton asymmetry can be measured through isospin-sensitive observables [3]. In summary, this is a timely and exciting topic, which is stimulating new effort, on both the experimental and the theoretical sides.

At this time, it is fair to say that the model dependence of the isospin asymmetric EOS is rather large. In fact, even the qualitative behavior of some predictions is controversial, as is the case, for instance, with the density dependence of the symmetry energy, upon which isospin diffusion in heavy-ion collisions is found to depend sensitively [4]. Thus any additional constraint is desirable and should be fully explored. As discussed in Ref. [5], nucleon-nucleus optical potential information can be exploited to constrain the strength and the energy dependence of the single-neutron and single-proton potentials in asymmetric nucler matter. The basic idea is that, even though infinite nuclear matter is an idealized system, the single-nucleon potentials should bear a clear signature of the optical potential in the interior of the nucleus.

In this paper we will concentrate specifically on predictions of the single-neutron and single-proton potentials and the closely related symmetry potential. For previous work on various aspects of the EOS in asymmetric matter we refer the reader to the bibliography of Ref. [7]. Unless otherwise specified, we use the Bonn-B potential [6] and the relativistic Brueckner-Hartree-Fock (DBHF) model outlined in Ref. [7]. We will compare with other predictions from the literature as well as empirical optical potential information. We will point out the large model dependence of predictions for those observables that depend sensitively on the difference between neutron and proton properties in asymmetric matter. Additional experimental constraints are therefore important. Moreover, microscopic, parameter-free approaches are the best way to gain deeper insight into the isospin-dependent properties of nuclear matter.

II. THE SINGLE-NUCLEON POTENTIALS

A. Momentum dependence

For the single-particle potential, we use the prescription of Refs. [8,9]. In the case of unequal Fermi levels for protons and neutrons, that prescription gives, schematically

$$U_i(k) = \mathrm{Re}\left[\sum_{q<k_F^n}\langle kq|G_{in}|kq-qk\rangle + \sum_{q<k_F^p}\langle kq|G_{ip}|kq-qk\rangle\right] \tag{1}$$

where $i = n/p$ for neutron/proton, and k refers to states below and above the Fermi momentum.

We begin by examining the momentum dependence of $U_{n/p}$, the single neutron and single-proton potential in neutron-rich matter. In Fig. 1, we show $U_{n/p}$ as a function of the momentum and for different values of the asymmetry parameter, $\alpha = (\rho_n - \rho_p)/(\rho_n + \rho_p)$, with ρ_n and ρ_p the neutron and proton densities. The total nucleon density considered in the figure is equal to 0.185 fm^{-3} and corresponds to a Fermi momentum of 1.4 fm^{-1}, which is very close to our predicted saturation density.

 ©2005 The American Physical Society

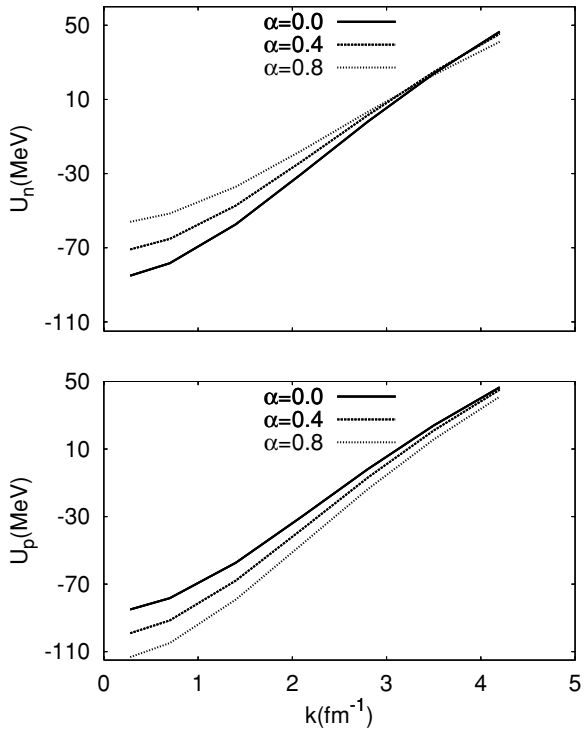

FIG. 1. The single-neutron (upper panel) and single-proton (lower panel) potential as a function of the nucleon momentum for three different values of the asymmetry parameter. The average Fermi momentum is 1.4 fm^{-1}.

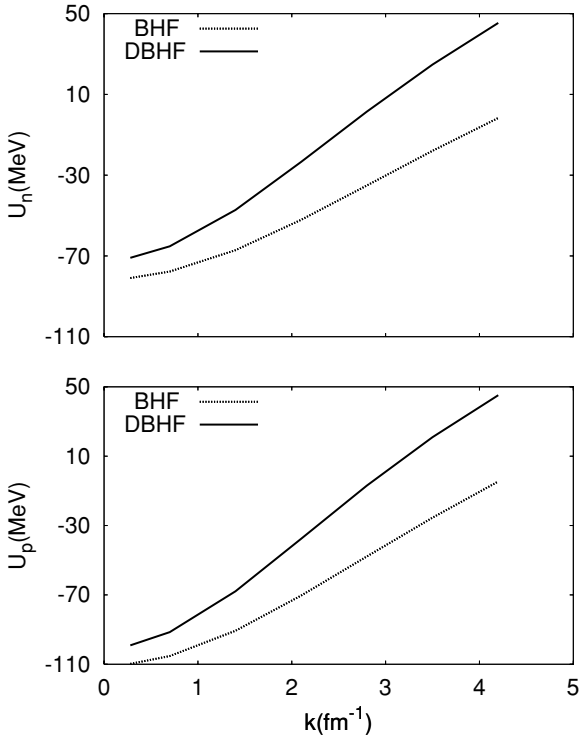

FIG. 2. Comparison between DBHF and BHF predictions of the single-neutron (upper panel) and single-proton (lower panel) potential. The value of the asymmetry parameter is fixed to 0.4 and the average Fermi momentum is 1.4 fm^{-1}.

For increasing values of α, the proton potential becomes increasingly attractive while the opposite tendency is observed in U_n. This reflects the fact that the proton-neutron interaction, the one predominantly felt by the single proton as the proton density is depleted, is more attractive than the one between identical nucleons. Also, as it appears reasonable, the dependence on α becomes weaker at larger momenta.

In Fig. 2 we show the DBHF results in comparison with those from (nonrelativistic) conventional Brueckner-Hartree-Fock (BHF) calculations. We make the comparison to show the considerable difference between the two sets of results as well as to check that our BHF predictions are in qualitative agreement with other studies based on the conventional Brueckner G-matrix approach. An older work based on that approach can be found, for instance, in Ref. [10], where separable representations of the nucleon-nucleon interaction are adopted. More recent calculations have been reported in Ref. [11], where the CD-Bonn potential [12] is used in conjunction with the BHF approximation.

The role of the momentum dependence of the symmetry potential in heavy-ion collisions was recently examined [13] and found to be important. Symmetry potentials with and without momentum dependence and yielding similar predictions for the symmetry energy can lead to significantly different predictions of collision observables [13].

B. Asymmetry dependence and the symmetry potential

Regarding $U_{n/p}$ as functions of the asymmetry parameter α, one can easily verify that the following approximate relation applies:

$$U_{n/p}(k, k_F, \alpha) \approx U_{n/p}(k, k_F, \alpha = 0) \pm U_{\rm sym}(k, k_F)\alpha \qquad (2)$$

with the $\pm$ referring to neutron/proton, respectively. Figure 3 displays the left-hand side of Eq. (1) for fixed density and nucleon momentum and clearly reveals the linear behavior of $U_{n/p}$ as a function of α.

Although the main focus of Fig. 3 is the α dependence, predictions are displayed for the Bonn A, B, and C potentials [6]. These three models differ mainly in the strength of the tensor force, which is mostly carried by partial waves with isospin equal to 0 and thus should fade away in the single-neutron potential as the neutron fraction increases. Reduced differences among the three models are in fact observed in U_n at the larger values of α.

Already several decades ago, it was pointed out that the real part of the nuclear optical potential depends on the asymmetry parameter as in Eq. (2) [14]. Thus, the quantity

$$\frac{U_n + U_p}{2} = U_0, \qquad (3)$$

which is obviously the single-nucleon potential in absence of asymmetry, should be a reasonable approximation to the isoscalar part of the optical potential. The momentum dependence of U_0 (which is shown in Fig. 1 as the $\alpha = 0$ curve), is important for extracting information about the symmetric matter EOS and is reasonably agreed upon [4,15–22].

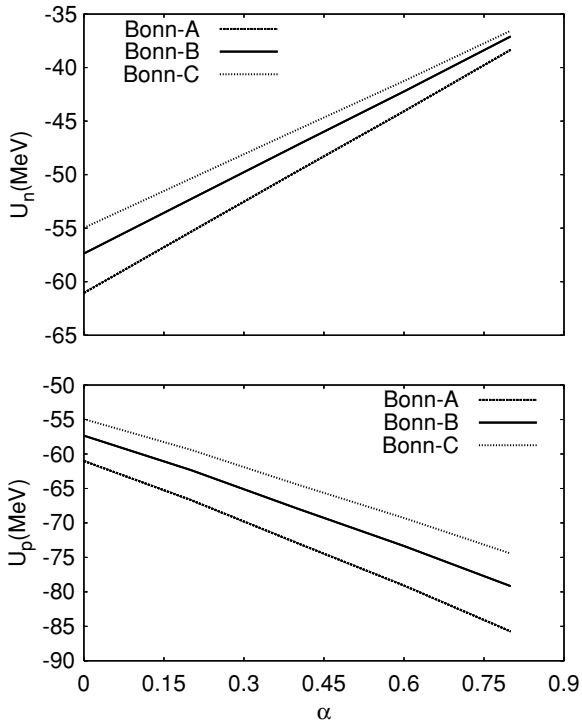

FIG. 3. The single-neutron (upper panel) and single-proton (lower panel) potential as a function of the asymmetry parameter for fixed average density ($k_F = 1.4\,\mathrm{fm}^{-1}$) and nucleon momentum ($k = k_F$).

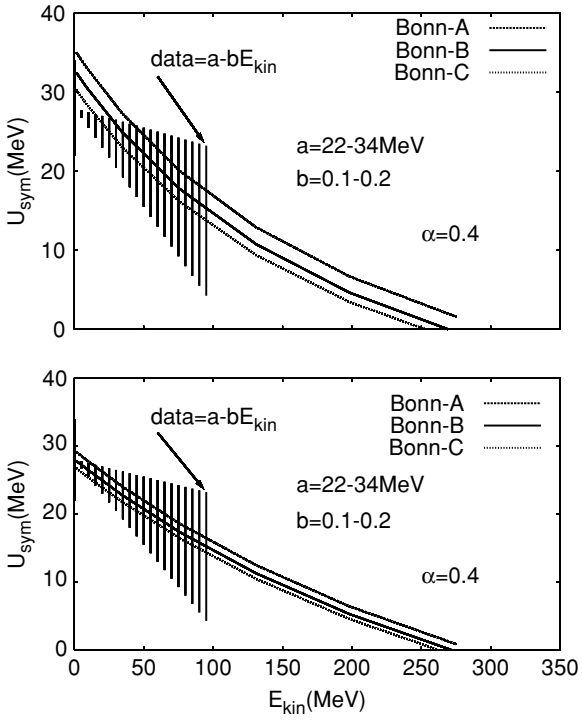

FIG. 4. The symmetry potential as a function of the nucleon kinetic energy close to saturation density (upper panel) and approximately one-half of saturation density (lower panel). The predictions obtained with Bonn A, B, and C are compared with empirical information from nuclear optical potential data (shaded area). See text for details.

On the other hand,

$$\frac{U_n - U_p}{2\alpha} = U_{\mathrm{sym}} \tag{4}$$

should be comparable with the Lane potential [14], or the isovector part of the nuclear optical potential. (Notice that in the two equations above the dependence upon density, momentum, and asymmetry has been suppressed for simplicity.) We have calculated U_{sym} as a function of the momentum, or rather the corresponding kinetic energy. The predictions obtained with Bonn A, B, and C are shown in Fig. 4. They are compared with the phenomenological expression [14]

$$U_{\mathrm{Lane}} = a - bT, \tag{5}$$

where T is the kinetic energy, $a \approx 22-34$ MeV, $b \approx 0.1-0.2$ MeV. We include in the figure predictions near saturation density ($k_F = 1.3\,\mathrm{fm}^{-1}$), and at a lower density ($k_F = 1.1\,\mathrm{fm}^{-1}$). The latter may be more appropriate when comparing with nuclear data. The differences between the upper and lower parts of Fig. 4 indicate that the density dependence is strongest at low momentum, as is reasonable. Furthermore, the model dependence is larger at the higher density. For completeness, we also show BHF predictions for the isovector potential, see Fig. 5. These are obtained with our standard choice for the *NN* potential, Bonn B, and at the same two densities considered in the previous figure. Comparison with the corresponding Bonn-B predictions from Fig. 4 reveals that the DBHF and the BHF predictions are very close. This can be understood noticing that the single-neutron and the single-proton potentials become more attractive by approximately the same amount in the BHF model, see Fig. 2, and thus their difference shows only minor variations. (We would not suggest, however, that the two models are equally valid, as other constraints clearly point to the DBHF model as more realistic.)

We observe that the strength of the predicted symmetry potential decreases with energy, a behavior which is consistent with the empirical information. The same comparison is done

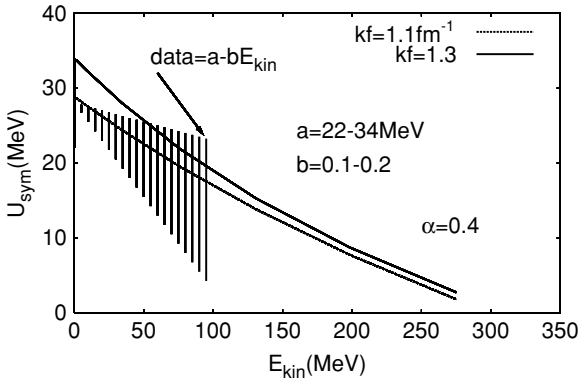

FIG. 5. As in Fig. 4, with the BHF model and the Bonn B potential. The corresponding Fermi momenta are indicated inside the figure.

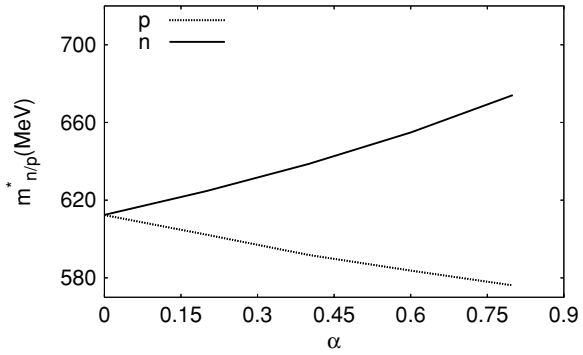

FIG. 6. The proton and neutron effective mass as a function of the asymmetry parameter and for fixed average density ($k_F = 1.4\,\mathrm{fm}^{-1}$).

in Ref. [5] starting from a phenomenological formalism for the single-nucleon potential [23,24]. There, it is shown that it is possible to choose two sets of parameters which lead to similar values of the symmetry energy but exactly opposite tendencies in the energy dependence of the symmetry potential as well as opposite sign of the proton-neutron mass splitting. As a consequence of that, these two sets of parameters lead to very different predictions for observables in heavy-ion collisions induced by neutron-rich nuclei [24]. This fact suggests that the parameters of the single-nucleon potential in asymmetric matter are weakly correlated to observables such as the energy per particle or the symmetry energy, where proton and neutron contributions are averaged together. Constraints from "differential" or relative observables, namely those specifically sensitive to the difference between proton and neutron properties, are thus very much needed [24].

The effective masses for proton and neutron corresponding to the single-nucleon potentials of Fig. 1 are shown in Fig. 6 as a function of α. The predicted effective mass of the neutron being larger than the proton's is a trend shared with microscopic nonrelativistic calculations [10]. In the nonrelativistic case, one can show from very elementary arguments based on the curvature of the single-particle potential that a more attractive potential, as the one of the proton, leads to a smaller effective mass. In our DBHF effective-mass approximation, we assume momentum-independent nucleon self-energies, U_S and U_V, with a vanishing spacial component of the vector part. In such limit, following similar calculations of symmetric matter [25], the one-body potential is written as [7]

$$U_i(p) = \frac{m_i^*}{E_i^*} U_{S,i} + U_{V,i}, \tag{6}$$

where $E_i^* = \sqrt{(m_i^*)^2 + p^2}$, $m_i^* = m_i + U_{S,i}$, and $i = n$ or p for neutrons or protons, respectively. Defining for convenience $U_{0,i} = U_{S,i} + U_{V,i}$, the expression above becomes a two-parameter formula which requires the fitting of two constants, just like in the nonrelativistic case. Now, since the single-proton potential is more attractive (see Fig. 1), and both the neutron and proton potentials tend to the same limit at high momenta, it is easy to see from Eq. (6), or rather its derivative, that the proton effective mass obtained in this way must be smaller than the neutron's.

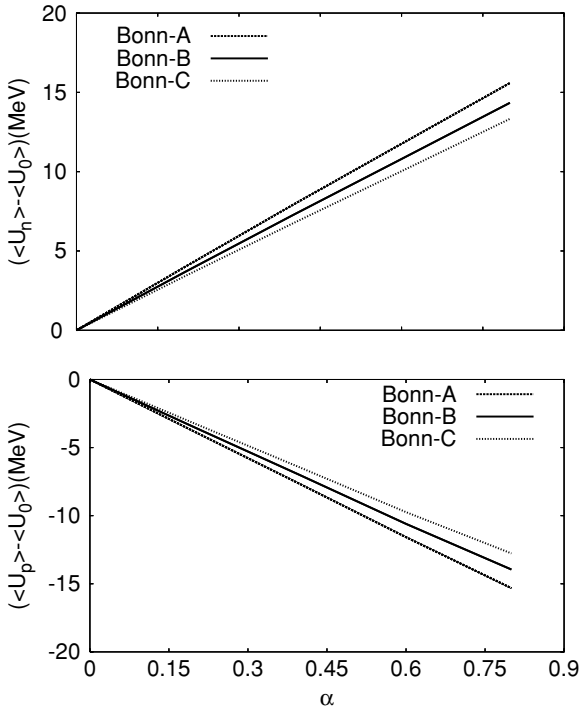

FIG. 7. Contribution from the asymmetry to the average potential energy per neutron (upper panel) and proton (lower panel). Average density as in the previous figures.

Before closing, we also show for completeness the average potential energy per neutron/proton, where the momentum dependence has been integrated out, see Fig. 7. This is the proton/neutron potential energy contribution to the total energy per particle which then appears in the EOS. Actually, what we show in Fig. 7 are the average potential energies from which the part coming from the symmetric EOS has been subtracted out, that is, just the contribution from the asymmetry to the interaction potential energy,

$$\langle \Delta U_{n/p} \rangle(\rho, \alpha) = \langle U_{n/p} \rangle(\rho, \alpha) - \langle U(\rho, \alpha = 0) \rangle. \tag{7}$$

Clearly, the contribution from the asymmetry, in both the momentum-dependent and the momentum-averaged potentials, turns out to be large and positive for neutrons, large and negative for protons. This component of the mean field will then be effective in separating the collision dynamics for neutrons and protons by making more neutrons unbound than protons (or, by making the neutrons more energetic, if already unbound). This effect can be discerned through observables such as the neutron/proton differential flow in heavy-ion collisions [3].

III. CONCLUSIONS

We have focused on some of the properties of neutrons and protons in neutron-rich matter. This is a topic of contemporary interest. Its relevance extends from the dynamics of colliding nuclei to nuclear astrophysics.

Different models may be in fair agreement with respect to averaged properties of the EOS, and yet produce very different

predictions of properties such as the symmetry potential and the closely related single-nucleon potentials and effective masses. Clearly, more stringent constraints are needed for the isospin-dependent properties of the EOS.

Very good transport model calculations are available from the literature [2,3]. However, a considerable amount of phenomenology is often involved in the input of these models (for instance, the mean field is based on some phenomenological interaction [13,26] and/or the elementary cross sections are obtained from empirical data). We calculate all of the above ingredients *microscopically* and internally consistent with respect to the two-body force. We are presently studying the dependence on density *and* asymmetry of the in-medium isospin-dependent nucleon-nucleon cross sections with the purpose of obtaining a convenient parametrization as a function of energy, density, and asymmetry. Our microscopic information (both elementary cross sections and mean field) can be a valuable input for transport model calculations of heavy-ion dynamical observables. This combined effort will complement new data to be taken at RIA and eventually shed light on the less known aspects of the nuclear equation of state.

ACKNOWLEDGMENT

The authors acknowledge financial support from the U.S. Department of Energy under Grant No. DE-FG02-03ER41270.

[1] D. Alonso and F. Sammarruca, Phys. Rev. C **68**, 054305 (2003).
[2] See, for instance, B. A. Li, Phys. Rev. Lett. **85**, 4221 (2000), and references therein.
[3] B. A. Li, C. M. Ko, and Z. Ren, Phys. Rev. Lett. **78**, 1644 (1997); B. A. Li, *ibid.* **88**, 192701 (2002).
[4] L.-W. Chen, Ch. M. Ko, and B.-A. Li, Phys. Rev. C **69**, 054606 (2004).
[5] B. A. Li, Phys. Rev. C **69**, 064602 (2004).
[6] R. Machleidt, Adv. Nucl. Phys. **19**, 189 (1989).
[7] D. Alonso and F. Sammarruca, Phys. Rev. C **67**, 054301 (2003).
[8] J.-P. Jeukenne, A. Lejeune, and C. Mahaux, Nucl. Phys. **A245**, 411 (1975).
[9] C. Mahaux, Nucl. Phys. **A328**, 24 (1979).
[10] I. Bombaci and U. Lombardo, Phys. Rev. C **44**, 1892 (1991).
[11] Kh. S. A. Hassaneen and H. Müther, Phys. Rev. C **70**, 054308 (2004).
[12] R. Machleidt, Phys. Rev. C **63**, 024001 (2001).
[13] B.-A. Li, C. B. Das, S. Das Gupta, and C. Gale, Phys. Rev. C **69**, 011603(R) (2004).
[14] A. M. Lane, Nucl. Phys. **35**, 676 (1962).
[15] C. Gale, G. Bertsch, and S. Das Gupta, Phys. Rev. C **35**, 1666 (1987).
[16] G. M. Welke, M. Prakash, T. T. S. Kuo, S. Das Gupta, and C. Gale, Phys. Rev. C **38**, 2101 (1988).
[17] C. Gale, G. M. Welke, M. Prakash, S. J. Lee, and S. Das Gupta, Phys. Rev. C **41**, 1545 (1990).
[18] Q. Pan and P. Danielewicz, Phys. Rev. Lett. **70**, 2062 (1993).
[19] J. Zhang, S. Das Gupta, and C. Gale, Phys. Rev. C **50**, 1617 (1994).
[20] V. Greco, A. Guarnera, M. Colonna, and M. Di Toro, Phys. Rev. C **59**, 810 (1999).
[21] P. Danielewicz, Nucl. Phys. **A673**, 375 (2000).
[22] D. Persram and C. Gale, Phys. Rev. C **65**, 064611 (2002).
[23] I. Bombaci, in *Isospin Physics in Heavy-Ion Collisions at Intermediate Energies*, edited by B. A. Li and W. Udo Schröder (Nova Science New York, 2001), Chap. 2.
[24] J. Rizzo *et al*., Nucl. Phys. **A732**, 202 (2004).
[25] R. Brockmann and R. Machleidt, Phys. Lett. **B149**, 283 (1984); Phys. Rev. C. **42**, 1965 (1990)
[26] C. B. Das, S. Das Gupta, C. Gale, and B.-A. Li, Phys. Rev. C **67**, 034611 (2003).